

Dose assessment for the fetus considering scattered and secondary radiation from photon and proton therapy when treating a brain tumor of the mother

Changran Geng^{1,2}, Maryam Moteabbed^{1,5}, Joao Seco^{1,5},
Yiming Gao³, X George Xu³, José Ramos-Méndez⁴,
Bruce Faddegon⁴ and Harald Paganetti^{1,5}

¹ Department of Radiation Oncology, Massachusetts General Hospital, Boston, MA 02114, USA

² Department of Nuclear Science and Engineering, Nanjing University of Aeronautics and Astronautics, Nanjing 210016, People's Republic of China

³ Nuclear Engineering Program, Rensselaer Polytechnic Institute, Troy, NY 12180, USA

⁴ Department of Radiation Oncology, University of California at San Francisco, CA 94143, USA

⁵ Harvard Medical School, Boston, MA 02114, USA

E-mail: geng.chr@gmail.com and HPAGANETTI@mg.harvard.edu

Received 9 September 2015, revised 4 December 2015

Accepted for publication 8 December 2015

Published 30 December 2015



CrossMark

Abstract

The goal of this work was to determine the scattered photon dose and secondary neutron dose and resulting risk for the sensitive fetus from photon and proton radiotherapy when treating a brain tumor during pregnancy. Anthropomorphic pregnancy phantoms with three stages (3-, 6-, 9-month) based on ICRP reference parameters were implemented in Monte Carlo platform TOPAS, to evaluate the scattered dose and secondary neutron dose and dose equivalent. To evaluate the dose equivalent, dose averaged quality factors were considered for neutrons. This study compared three treatment modalities: passive scattering and pencil beam scanning proton therapy (PPT and PBS) and 6-MV 3D conformal photon therapy. The results show that, for 3D conformal photon therapy, the scattered photon dose equivalent to the fetal body increases from 0.011 to 0.030 mSv per treatment Gy with increasing stage of gestation. For PBS, the neutron dose equivalent to the fetal body was significantly lower, i.e. increasing from 1.5×10^{-3} to 2.5×10^{-3} mSv per treatment Gy with increasing stage of gestation. For PPT, the neutron dose equivalent of the fetus decreases from 0.17 to 0.13 mSv per treatment Gy

with the growing fetus. The ratios of dose equivalents to the fetus for a 52.2 Gy(RBE) course of radiation therapy to a typical CT scan of the mother's head ranged from 3.4–4.4 for PBS, 30–41 for 3D conformal photon therapy and 180–500 for PPT, respectively. The attained dose to a fetus from the three modalities is far lower than the thresholds of malformation, severe mental retardation and lethal death. The childhood cancer excessive absolute risk was estimated using a linear no-threshold dose-response relationship. The risk would be 1.0 (95% CI: 0.6, 1.6) and 0.1 (95% CI: –0.01, 0.52) in 10^5 for the 9-month fetus for PBS with a prescribed dose of 52.2 Gy(RBE). The increased risks for PPT and photon therapy are about two and one orders of magnitude larger than that for PBS, respectively. We can conclude that a pregnant woman with a brain tumor could be treated with pencil beam scanning with acceptable risks to the fetus.

Keywords: proton therapy, Monte Carlo, computational phantom, fetus dose

(Some figures may appear in colour only in the online journal)

1. Introduction

About one in a thousand pregnant women are diagnosed with cancer (Pavlidis 2002). When the treatment cannot be postponed post pregnancy, decisions need to be made regarding the use of surgery, chemotherapy and/or radiation therapy and the potential impact on the fetus (Willemse *et al* 1990, Pavlidis 2002, Weisz *et al* 2004, Pentheroudakis and Pavlidis 2006). Radiation therapy, as one of three main methods of cancer therapy, plays an important role in the treatment for pregnant women (Stovall *et al* 1995, Greskovich and Macklis 2000, Magne *et al* 2001, Wo and Viswanathan 2009). While many cancers would not be treated with radiation during pregnancy, brain tumors might be considered due to the relatively large distance to the fetus (Magne *et al* 2001). Proton therapy offers an advantage because of the reduced integral dose (Paganetti *et al* 2012, Moteabbed *et al* 2014). Nevertheless, scattered and secondary radiation from both proton and photon treatment delivery systems and produced in the mother's body could be a potential risk for the radiosensitive fetus (Schneider *et al* 2002, Jiang *et al* 2005, Hall 2006, Jarlskog *et al* 2008). The potential risks include mental retardation, microcephaly, growth retardation, cancer, and even lethality in utero.

Many investigators and organizations studied the scattered dose to the fetus from conventional x-ray therapy. The Task Group 36 of the American Association of Physicists in Medicine (AAPM) recommended procedures and methods to estimate the fetal dose from photon therapy. The scattered fetal dose estimated by the TG-36 recommendation was evaluated with measurement using field sizes different from the TG-36 recommendation for specific tumors (Kry *et al* 2007). Bednarz *et al* calculated the fetus dose for the similar scenario as Kry *et al* using the computational phantoms and Monte Carlo method (Bednarz and Xu 2008). Horowitz *et al* reported cumulate fetal doses of 0.04 Gy and 0.026 Gy during a course of 60 Gy to the target without and with shielding, respectively, for a case of IMRT for glioblastoma (Horowitz *et al* 2014).

Few studies were performed on the dose to a fetus from proton therapy during pregnancy by measurement or simulation. Attaching a water or solid phantom to a physical anthropomorphic phantom, and determining the fetal dose using point-dose measurements is a potentially

Table 1. Beam configurations for PPT and PBS treatment plan.

	Beam1	Beam2	Beam3	Beam4	Beam5
Gantry angle (degree)	240	180	120	240	180
Range (mm)	101	112	136	101	112
Air gap (mm)	30	35	35	30	35

valid approximation (Bednarz and Xu 2008). Mesoloras *et al* measured the neutron dose equivalent to a fetus from passive scattering using a Rando phantom enhanced by a wax bolus to mimic the second trimester pregnancy (Mesoloras *et al* 2006). They placed a neutron bubble detector 10 cm below the umbilicus in the phantom to represent the fetus position. They measured the neutron dose equivalent to the fetus with decreasing distance to field edge from 61.4 to 4.4 cm and found that it varied from 0.025 to 0.450 mSv per treatment Gy for a small field snout and from 0.097 to 0.871 mSv per treatment Gy for a large field snout. They also concluded that the neutron dose equivalent increased with incident proton energy and decreased with aperture size, distance of the fetus representative point from the field edge, and increasing air gap.

Our study goes one step further in investigating the scattered and secondary fetal doses and risks in different stages from proton therapy with passive scattering (PPT), pencil beam scanning (PBS), as well as photon therapy, considering patients receiving treatment for a brain tumor. A robust dose assessment procedure was constructed applying three computational phantoms representing 3-month, 6-month and 9-month pregnancy implemented into the Monte Carlo platform TOPAS and link the phantom geometry to a specific treatment plan. For proton therapy, the organ specific dose equivalent was estimated by dose averaged linear energy transfer (LET)-based quality factors following the recommendations by the International Commission on Radiological Protection (ICRP). The LET refers to the local energy deposition of charged particle per unit length.

2. Methods and materials

2.1. Treatment delivery and planning

The delivery systems considered in the simulations are the Francis H Burr Proton Therapy Center at Massachusetts general hospital (MGH) for proton therapy, a Varian 2100 photon LINAC and a Siemens Oncor LINAC for photon therapy. The passive scattering and pencil beam scanning plans with five fields were created and optimized for a brain tumor patient using the XIO (CMS Inc., St. Louis, Missouri) and ASTROID (MGH in-house developed) treatment planning systems, respectively. For pencil beam scanning, the spot size is ~10 mm and no patient-specific aperture applied. The prescribed dose was assumed to 52.2 Gy(RBE). The assumed tumor size was $6.5 \times 6.5 \times 4.5 \text{ cm}^3$ treated with single-field uniform dose. The configurations of the beams are listed in table 1. Because of the radial symmetry of the problem (the fetus being orthogonal to the beam direction) and the proton treatment plans relying mainly on posterior fields, for 6 MV 3D conformal radiation therapy (3D-CRT), a single beam $6.5 \times 4.5 \text{ cm}^2$ in size from the posterior direction was considered.

2.2. Whole body computational pregnancy phantoms

In order to model the body during pregnancy including the fetal anatomy, a series of phantoms was developed using a boundary representation (BREP) modeling approach as shown

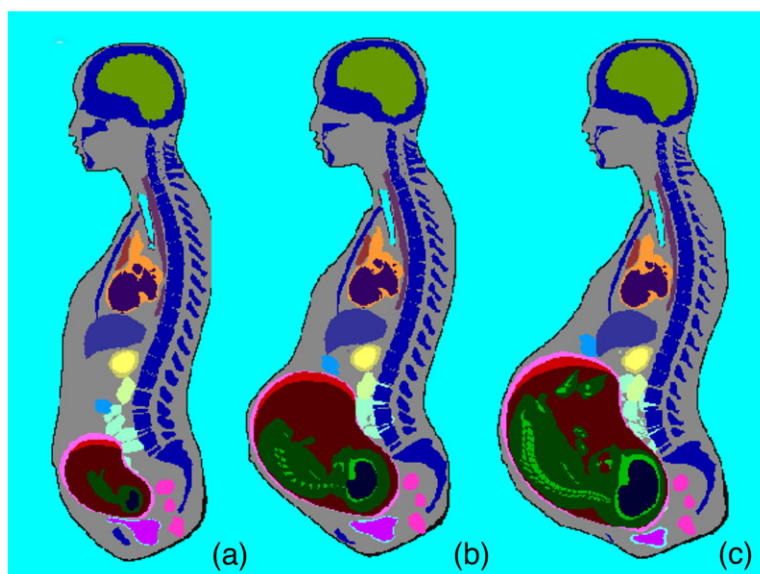


Figure 1. RPI- Pregnant phantom in the stage of (a) 3-month, (b) 6-month and (c) 9-month (Xu *et al* 2007).

in figure 1 (Xu *et al* 2007). These phantoms include a pregnant female and her fetus at the end of three gestational periods, i.e. 3-, 6- and 9-month, respectively. The organ masses in the phantom were defined in agreement with the reference data recommended by the ICRP. The phantoms distinguish 31 organs for the mother as well as fetal brain and fetal soft tissue for the fetus in the stage of 3-month and fetal brain, fetal skeleton and fetal brain for the fetuses in the stage of 6- and 9-month.

2.3. Dose equivalent

The difference in the biological effectiveness of radiations was considered by applying the quality factor as recommended by the ICRP in 1990 (ICRP 1991). In ICRP report 103, it was recommended to change practice by using the radiation weighting factor concept instead (ICRP 2007). However, the radiation weighting factor corresponds to an external field and one type of radiation only. The applicability of the radiation weighting factor for risk assessment in external beam radiation therapy is unclear (ICRP 2003b, Xu and Paganetti 2010). On the other hand, the quality factor (Q) is a continuous function of the LET at the organ position and thus accounts for external as well as internal radiation of different types. The latest recommendations for $Q(\text{LET})$ are provided in ICRP report 60 (ICRP 1991). Because this recommended relationship is defined in water, density corrections were used to determine the LET values in different tissues in TOPAS. The mean quality factor in an organ is determined by averaging over organ mass and absorbed dose,

$$Q_T = \frac{1}{m_T D_T} \int_{m_T} \int_{\text{LET}=0}^{\text{LET}=\infty} Q(\text{LET}) D(\text{LET}) d\text{LET} dm \quad (1)$$

where m_T stands for the mass in tissue T and D_T represents the mean dose in the tissue T .

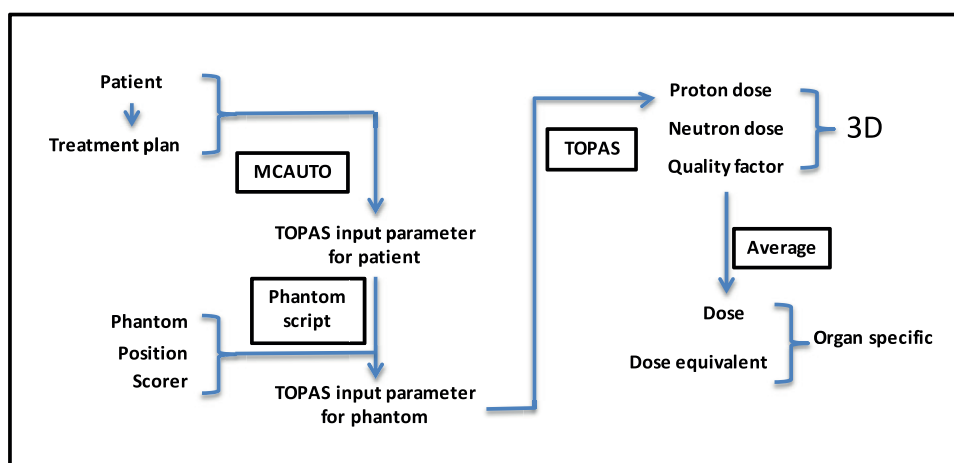


Figure 2. Flow chart for the estimation of neutron dose and dose equivalent in proton therapy using TOPAS. MCAUTO is a script connecting the treatment planning environment with the Monte Carlo environment. The phantom script replaces the patient geometry by a phantom geometry at the relative position and adds a scorer, which is a function called by the user to record a specific simulation property.

2.4. TOPAS (TOol for Particle Simulation) and configuration

TOPAS is an innovative Monte Carlo research platform for radiation therapy based on the Monte Carlo toolkit Geant4 (Perl *et al* 2012). For proton therapy, an in-house script was used to readout the treatment plan information from the treatment planning system. This is routinely done for patient dose calculation at our institution (Schuemann *et al* 2014). The treatment head simulation has been previously validated against measurement (Testa *et al* 2013). The patient geometry of a representative patient with brain tumor was replaced by phantom geometry while maintaining the treatment plan information.

For photon therapy, we generated phase space files with field size of $10 \times 10 \text{ cm}^2$ and $6.5 \times 4.5 \text{ cm}^2$, which is the tumor size considered in this study, using the BEAMnrc code (Rogers *et al* 1995). The simulations were previously validated with measurement (Seco *et al* 2005, Sawkey and Faddegon 2009). The phase space data includes primary and scattered photons and charged particles from the treatment head, but not leakage. The phase space files were translated into the format recognized by TOPAS. A water tank was modeled to get the depth dose distribution with the phase space file of $10 \times 10 \text{ cm}^2$ and 90 cm source-to-surface distance. A scaling factor was applied to the reference point at 10 cm depth, to convert the calculated dose to dose per treatment Gy. The fetus doses for photon therapy were averaged considering the doses from a Siemens and a Varian LINAC.

Subsequently, organ specific dose and dose equivalent calculations were based on 3D dose distributions from TOPAS. Figure 2 shows the workflow for the estimation of neutron dose and dose equivalent in proton therapy using TOPAS. Figure 3 shows the positioning of a phantom in TOPAS, as well as the comparison of calculated dose distribution based on the phantom and patient geometry. Different numbers of initial particles were considered for each modality to ensure a statistical uncertainties of organ doses below 5%. For PBS, 2×10^8 primary protons were simulated for each beam. For PPT, 4×10^9 primary protons were simulated for each beam. For photon therapy, 1×10^{12} primary electrons were simulated for each beam.

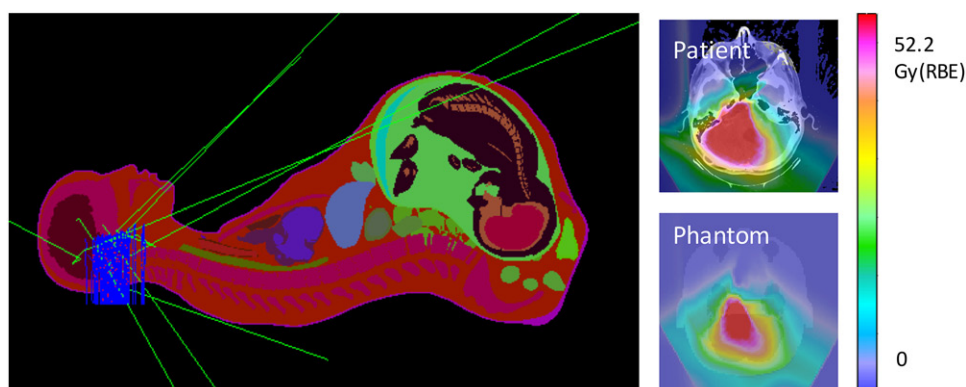


Figure 3. Illustration of the phantom geometry and positioning in TOPAS and comparison of calculated proton dose distributions in the brain based on phantom and patient geometry. In the left panel, the blue lines represent the primary proton tracks, and the green lines represent the secondary neutrons.

2.5. CT dose calculation

In order to compare the fetal dose for radiation therapy to that for a CT scan, we calculated the fetal dose for a CT scan of the mother's head using VirtualDose, which is a commercial software developed for CT dose evaluation (Ding *et al* 2015). The CT scanner simulated was GE LightSpeed Pro 16. The protocol followed the routine brain CT scan. The doses for three stages were calculated with the tube voltage of 120 kVp and the tube current of 200 mA for 0.5 s rotational time (see figure 6(b)).

3. Results

3.1. Dose equivalents for fetus in proton and photon therapy

Figure 4 shows the scattered photon dose and neutron dose equivalent for the three fetuses in different stages from three treatment modalities. For PBS, the mean neutron dose equivalent to the whole fetus increases from 1.5×10^{-3} to 2.5×10^{-3} mSv per treatment Gy with increasing stage of gestation. For the passive scattering technique, the mean neutron dose equivalent to the whole fetus shows a decrease from 0.17 to 0.13 mSv per treatment Gy with the fetus grows. For the 3D-CRT technique, the doses from the two different LINACs are very close. The scattered photon doses are 0.011, 0.024 and 0.030 mSv per treatment Gy. This shows a similar trend for different stages compared to PBS albeit one order of magnitude higher. Leakage dose is not included for photon therapy and would increase the dose, although in practice this would be much lower than the scattered dose due to the shielding by primary and secondary collimation in the patient plane (Chofor *et al* 2012).

Comparing our results for photon therapy to those in Chofor *et al* the total scatter dose (from treatment head and patient) at 50 cm for a 5×5 cm² field size and 6 MV photons is about 0.02 mSv Gy⁻¹ (Chofor *et al* 2012), which is consistent with our results. However, there is a difference when comparing to data from AAPM TG36, where the dose is ~ 0.2 mSv Gy⁻¹ for field size of 5×5 cm² and 6 MV photons. This difference can be attributed to the difference in manufacturer and potential background/leakage radiation during the measurement (Stovall *et al* 1995).

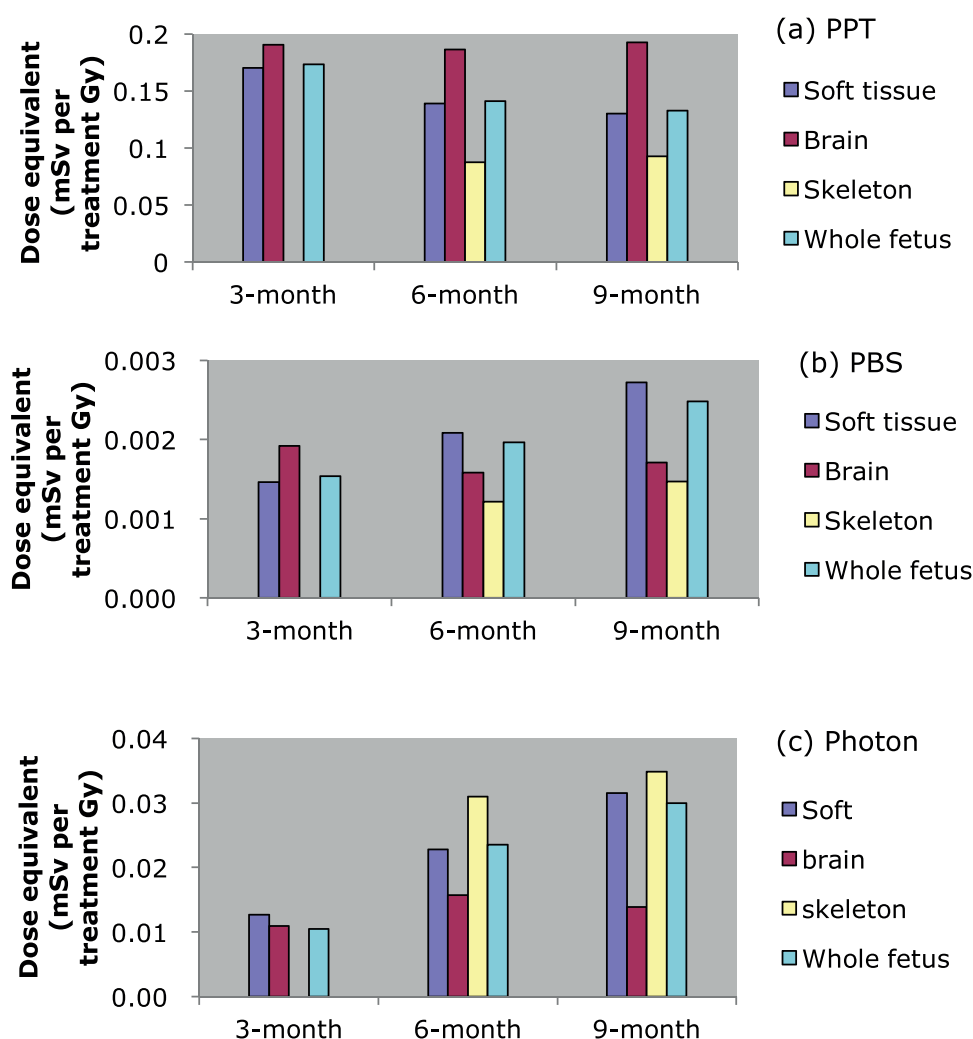


Figure 4. Dose equivalents (mSv per treatment Gy) averaged over organs and the whole body of the fetus for three stages for proton therapy ((a) PPT, (b) PBS) and (c) photon therapy (average considering a Varian and Siemens LINAC). Note that the skeleton dose for 3-month is 0 because no skeleton exists in the 3-month fetus phantom.

The mean quality factors for the whole fetus are 4.1, 3.7, and 3.6 for the 3-, 6-, 9-month phantoms in PPT, respectively. For PBS, the mean quality factors are 4.4, 4.3, and 4.4. Mean quality factors of unity are assumed for the 6 MV photon treatments.

The dose distributions in the sagittal plane for different fetus stages are shown in figure 5. For PBS and photon therapy, the dose equivalent profile of the fetus is independent of the beam direction, if it is orthogonal to the patient axis (head to foot), and only depends on the distance from the target, i.e. the brain of the mother in this study. On the other hand, for PPT, the dose equivalent strongly depends on the beam direction. This is because the majority of secondary radiation in PPT originates from the treatment head.

The mean fetal dose for one CT scan of the mother's head is increased from 0.018 to 0.038 mGy with the growing fetus (figure 6). Table 2 tabulates the ratios of the dose received by the fetus

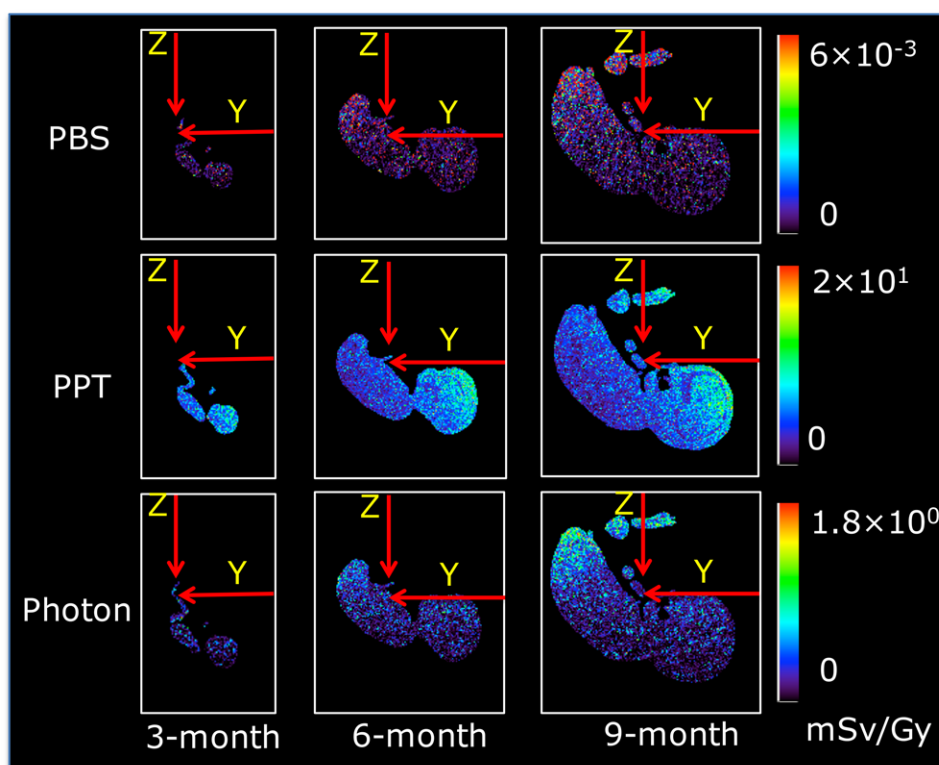


Figure 5. Dose equivalent profiles for PBS, PPT and photons (Varian LINAC) shown in the Sagittal plane. Note that the *Y* direction represents the posterior-anterior direction while the *Z* direction points from head to foot of the mother.

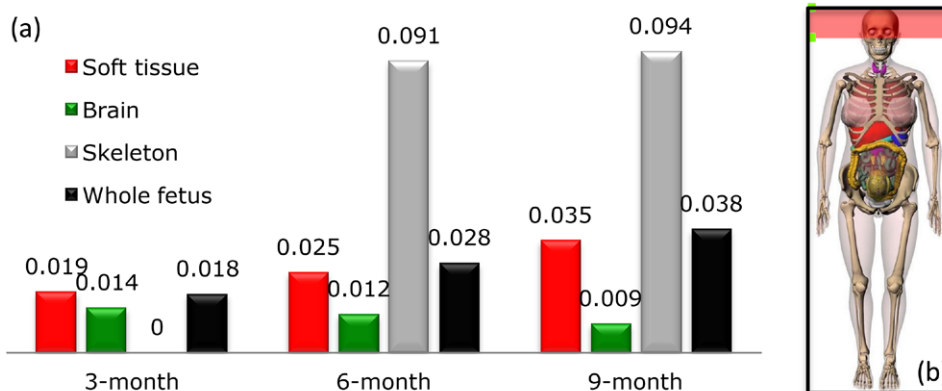


Figure 6. Left panel (a) shows the fetal doses (mGy) for a CT scan of the head of the mother. Right panel (b) shows the phantom with a 6-month fetus, and the scan in red shadow. Note that the skeleton dose for 3-month is 0 because no skeleton exists in the 3-month fetus phantom.

Table 2. Ratios of dose equivalent received by the fetus for radiation therapy with a prescribed dose of 52.2 Gy(RBE) divided by that of a CT scan of the mother's head (2 significant figures).

Stage	PPT	PBS	Photon
3 month	500	4.4	30
6 month	260	3.7	44
9 month	180	3.4	40

for radiation therapy with a prescribed dose of 52.2 Gy(RBE) divided by that of a CT scan of the mother's head.

4. Discussion

Scattered and secondary radiation from radiation therapy during pregnancy may cause a risk to the fetus. While this issue has been discussed in photon therapy, there are very few studies for proton therapy, although one might expect substantially different dose levels compared to photons, with PBS offering a chance to treat pregnant patients that were not considered previously for radiation therapy. Most of the experimental estimations were realized using solid water as the physical phantom and measuring doses at selected points. There are various limitations of this method, e.g. the dose is not uniformly distributed in most cases and there is no method to reasonably determine quality factors. This study used realistic computational phantoms and the well validated Monte Carlo toolkit TOPAS for the proton treatments and EGSnrc/BEAMnrc along with TOPAS for the photon treatments to calculate the beam details and evaluate the dose to a fetus.

4.1. Dose equivalent

Generally, the scattered or secondary dose consists of two parts. One is from the patient body while another is from the treatment delivery system. Comparing the two proton therapy modalities, PPT shows higher neutron doses to the fetus compared to PBS because of neutrons generated in the delivery system. Overall, the fetal doses from photon therapy are lower compared to PPT. As the fetus grows, the dose to soft tissue of the fetus increases due to the decreasing distance to the target region as the main scattered and secondary radiation to the fetus are generated in the patient for PBS and photon therapy. In contrast, for PPT the dose to the soft tissue decreases as the fetus grows. This is due to the decreased dose from the back part of the mother's body because the beams used in this study were posterior to the mother's head, as listed in table 1, and in PPT the main contribution of secondary and scattered radiation is from the treatment head. Given the rate of the dose-fall-off the average dose to the fetus may also increase with size of the fetus.

The skeleton dose equivalent is lower compared to soft tissue in both PPT and PBS while this is reversed for photon therapy. This is due to different energy deposition patterns of photons and secondary neutrons. The neutrons dominantly deposit energy by interaction with hydrogen in soft tissue via the (n,p) reaction, while photons deposit more energy in higher atomic number material, i.e. the skeleton, via the photoelectric effect.

The average fetal dose from the head CT scan increases as the fetus grows, again due to the closer proximity of the fetus to the irradiated volume. Comparing the dose to the fetus caused by a head CT scan of the mother, as shown in table 2, the mean dose equivalents of the whole

fetal body are only 3.4–4.4 times larger for PBS with a prescribed dose of 52.2 Gy(RBE). For photon therapy the factor ranges from 30 to 44 with the growing fetus whereas for PPT, the factors are highest due to the neutron component, i.e. decreasing from 500 to 180 with the growing fetus. Note there is no neutron component for the 6 MV x-ray treatment since the energy is below the threshold for photoneutron production.

Note that, compared to 3D-CRT, one would expect Intensity Modulated Radiation Therapy (IMRT) to result in about 80% higher scattered dose to out of field organs (Ruben *et al* 2011). Note also that only one case with a target size of $6.5 \times 6.5 \times 4.5 \text{ cm}^3$ was considered as representative in this study, the dose values could vary with different tumor sizes and sites for all modalities. One can expect that with larger tumor size the dose equivalent for PBS and photon therapy would be larger since more radiation fluence is needed to cover the tumor for all the three modalities. On the other hand, a larger field size could reduce the neutron dose in PPT because of the decreasing aperture blocking. Furthermore, higher proton energies needed to reach a deeper target for PPT and PBS could increase in-patient neutron production (Zacharatou Jarlskog *et al* 2008).

Although the established quality factor for neutron radiation was used in this study, the relationship of biological effects and radiation quality still has considerable uncertainties. Based on the ICRP recommendations, the radiation weighting factor varies as a function of energy with a maximum value of 20 at 1 MeV. However, in the context of secondary neutrons from proton therapy, the neutron energy range is up to tens or hundreds of MeV where the weighting factor would be much lower. While the dosimetric aspects of neutrons are reasonably well understood, there is controversy regarding their biological effectiveness for epidemiologic endpoints (Kocher *et al* 2005, Brenner and Hall 2008).

4.2. Risk estimation

The side effects and risks from radiation of a fetus were summarized by several organizations, such as the AAPM (Stovall *et al* 1995), the ICRP (ICRP 2003a) and, more recently, the National Council on Radiation Protection and Measurements (NCRP 2013).

The Oxford Survey of Childhood Cancers (OSCC) and Japanese atomic epidemic studies provide the main data for the study of in-utero radiation effects. Although these studies have their limitations and the results have large uncertainties, several conclusions are valid. The nature and severity of induced biological effects depends on the developmental stage during which the radiation exposure takes place (Miller 1990, ICRP 2003a). Noncancerous health effects are not observed below a threshold of 0.05 Gy in all periods (ICRP 2000). During the period of pre-implantation, radiation exposure could result in a risk of failure to implant when the fetus receives dose larger than 0.1 Gy, and any other effects are not observed if the fetus can survive (Miller 1990, ICRP 1991). Malformation always takes place at the organogenesis period, and has a substantial risk when the exposure dose to the fetus is above 0.5 Gy (Lee *et al* 1999, ICRP 2003a). A verifiable decrease of intelligence quotient (IQ) is observed when the fetal dose exceeds about 0.1 Gy (ICRP 2000). For severe mental retardation, the 95% lower confidence bound on the threshold fetal dose is 0.3 Gy (ICRP 2003a).

The absorbed dose to the fetus from three modalities considered here is far lower than the thresholds for malformation, severe mental retardation (SMR) and lethality. Several models for childhood cancer risk estimation from fetal dose were introduced and are associated with large uncertainties (Wakeford and Little 2003). Two of the excess absolute risk coefficients for childhood cancer following radiation exposure based on incidence data from two different typical studies are listed in table 3 (Wakeford and Little 2003). The excess absolute risk for childhood cancer can be estimated using a linear no-threshold dose-response relationship.

Table 3. Excess absolute risk coefficients for childhood Cancer following radiation exposure based on incidence data under the age of 15-year-old.

	Model	EAR (95% CI), (% Gy ⁻¹)
All Cancers	Oxford survey of childhood cancers (case-control study)	8.0 (4.4,12) (Bithell 1993)
	Japanese atomic bomb survivors (cohort study)	0.8 (-0.1,4) (Wakeford and Little 2003)

For instance, PBS with the prescribed dose of 52.2 Gy(RBE) would increase the risk by 1.0 (95% CI: 0.6, 1.6) and 0.1 (95% CI: -0.01, 0.52) in 10^5 for the 9-month fetus using the OSCC and Japanese atomic model, respectively. For PPT the risks would be increased by 56 (95% CI: 31, 83) and 5.5 (95% CI: -0.7, 28) in 10^5 for the 9-month fetus. For photons, the increased risks are about one order of magnitude higher than those from PBS, i.e. 13 (95% CI: 6.9, 19) and 1.3 (95% CI: -0.15, 6.3) in 10^5 for the 9-month fetus. The baseline rate of the cancer incidence from birth to 15-year-old is 237 in 10^5 (Howlader *et al* 2015).

The risk models were mostly deduced with the third trimester, so the estimation for the first and second trimester is relatively conservative since the risk for the first trimester is higher than the third trimester (ICRP 2000).

5. Summary and conclusion

The implementation of computational phantoms into TOPAS to simulate equivalent doses for radiation protection purposes was demonstrated. Scattered and secondary doses to a fetus were calculated and compared for passive scattering, pencil beam scanning proton therapy and photon therapy for a brain tumor case. The dose equivalent received by the fetus body for pencil scanning beam proton therapy shows the lowest value, which is about 4 times higher than the fetal dose for one CT scan of mother's head. For photon therapy and PPT, the dose equivalents received by the fetus (excluding leakage dose for photons) are one and two orders of magnitude larger than that for PBS, respectively. When determining the fetal dose in different stages, the resulting dose from the secondary and scattered radiation depends on the distance from the target (for PBS and photon therapy). For neutrons originating in the treatment head the dose is less dependent on the distance from the target but more on the beam direction (for PPT).

The absorbed dose to a fetus from three modalities considered here is far lower than the thresholds of malformation, SMR and lethal death. The cancer excessive absolute risk for childhood cancer was estimated to be quite low comparing to the baseline cancer incidence.

We can conclude that, independent of the stage of pregnancy, radiation treatment for a brain tumor comes at a very low risk to the fetus, in particular if pencil beam scanning proton therapy is being used. For PPT, one should consider utilizing external neutron shielding material (such as Polyethylene) to reduce the risk from excess radiation, following the 'as low as reasonably achievable' principle.

Acknowledgments

CG was funded by the China Scholarship Council (CSC) and the National Natural Science Foundation of China (Grant No. 11475087). We would like to thank the MGH Monte Carlo group for many fruitful discussions and the Partners Research Computing group for maintaining the computer cluster.

References

- Bednarz B and Xu X G 2008 A feasibility study to calculate unshielded fetal doses to pregnant patients in 6 MV photon treatments using Monte Carlo methods and anatomically realistic phantoms *Med. Phys.* **35** 3054
- Bithell J F 1993 Statistical issues in assessing the evidence associating obstetric irradiation and childhood malignancy *Proc. New Evaluation of Radiation Hazard: Low-Dose Radiation and Health* ed E Lengfelder and H Wendhausen (Muruch: MMV Medizin Verlag) pp 53–60
- Brenner D J and Hall E J 2008 Secondary neutrons in clinical proton radiotherapy: A charged issue *Radiother. Oncol.* **86** 165–170
- Chofor N, Harder D, Willborn K C and Poppe B 2012 Internal scatter, the unavoidable major component of the peripheral dose in photon-beam radiotherapy *Phys. Med. Biol.* **57** 1733–43
- Ding A, Gao Y, Liu T, Caracappa P F, Long D J, Bolch W E, Liu B and Xu X G 2015 VirtualDose: a software for reporting organ doses from CT for adult and pediatric patients *Phys. Med. Biol.* **60** 5601–25
- Greskovich J F and Macklis R M 2000 Radiation therapy in pregnancy: risk calculation and risk minimization *Semin. Oncol.*
- Hall E J 2006 Intensity-modulated radiation therapy, protons, and the risk of second cancers *Int. J. Radiat. Oncol. Biol. Phys.* **65** 1–7
- Horowitz D P, Wang T J C, Wu C-S, Feng W, Drassinower D, Lasala A, Pieniazek R, Cheng S, Connolly E P and Lassman A B 2014 Fetal radiation monitoring and dose minimization during intensity modulated radiation therapy for glioblastoma in pregnancy *J. Neuro Oncol.* **120** 405–9
- Howlander N et al 2015 *SEER Cancer Statistics Review 1975–2012* (Bethesda, MD: National Cancer Institute)
- ICRP 1991 Recommendations of the international commission on radiological protection *ICRP Publication 60* (Oxford: Pergamon)
- ICRP 2000 Pregnancy and medical radiation *ICRP Publication 84* (Oxford: Pergamon)
- ICRP 2003a Biological effects after prenatal irradiation (embryo and fetus) *ICRP Publication 90* (Oxford: Pergamon)
- ICRP 2003b Relative biological effectiveness, radiation weighting and quality factor *ICRP Publication 92* (Oxford: Pergamon)
- ICRP 2007 The 2007 recommendations of the international commission on radiological protection *ICRP Publication 103* (Oxford: Pergamon)
- Jarlskog C Z, Lee C, Bolch W E and Xu X G 2008 Assessment of organ-specific neutron equivalent doses in proton therapy using computational whole-body age-dependent voxel phantoms *Phys. Med. Biol.* **53** 693–717
- Jiang H, Wang B, Xu X G, Suit H D and Paganetti H 2005 Simulation of organ-specific patient effective dose due to secondary neutrons in proton radiation treatment *Phys. Med. Biol.* **50** 4337–53
- Kocher D C, Apostoaei A I and Hoffman F O 2005 Radiation effectiveness factors for use in calculating probability of causation of radiogenic cancers *Health Phys.* **89** 3–32
- Kry S F, Starkschall G, Antolak J A and Salehpour M 2007 Evaluation of the accuracy of fetal dose estimates using TG-36 data *Med. Phys.* **34** 1193
- Lee S, Otake M and Schull W J 1999 Changes in the pattern of growth in stature related to prenatal exposure to ionizing radiation *Int. J. Radiat. Biol.* **75** 1449–58
- Magne N, Marcie S and Pignol J P 2001 Radiotherapy for a solitary brain metastasis during pregnancy: a method for reducing fetal dose *Br. J. Radiol.* **74** 638–41
- Mesoloras G, Sandison G A, Stewart R D, Farr J B and Hsi W C 2006 Neutron scattered dose equivalent to a fetus from proton radiotherapy of the mother *Med. Phys.* **33** 2479
- Miller R W 1990 Effects of prenatal exposure to ionizing radiation *Health Phys.* **59** 57–61
- Moteabbed M, Yock T I and Paganetti H 2014 The risk of radiation-induced second cancers in the high to medium dose region: a comparison between passive and scanned proton therapy, IMRT and VMAT for pediatric patients with brain tumors *Phys. Med. Biol.* **59** 2883–99
- NCRP 2013 Preconception and prenatal radiation exposure: health effects and protective guidance NCRP Report 174
- Paganetti H, Athar B S and Moteabbed M 2012 Assessment of radiation-induced second cancer risks in proton therapy and IMRT for organs inside the primary radiation field *Phys. Med. Biol.* **57** 6047–61
- Pavlidis N A 2002 Coexistence of pregnancy and malignancy *Oncologist* **7** 279–87

- Pentheroudakis G and Pavlidis N 2006 Cancer and pregnancy: poena magna, not anymore *Eur. J. Cancer* **42** 126–40
- Perl J, Shin J, Schümann J, Faddegon B and Paganetti H 2012 TOPAS: an innovative proton Monte Carlo platform for research and clinical applications *Med. Phys.* **39** 6818
- Rogers D W O, Faddegon B A, Ding G X, Ma C M, We J and Mackie T R 1995 BEAM: A Monte Carlo code to simulate radiotherapy treatment units *Med. Phys.* **22** 503–24
- Ruben J D, Lancaster C M, Jones P and Smith R L 2011 A Comparison of out-of-field dose and its constituent components for intensity-modulated radiation therapy versus conformal radiation therapy: implications for carcinogenesis *Int. J. Radiat. Oncol. Biol. Phys.* **81** 1458–64
- Sawkey D and Faddegon B A 2009 Simulation of large x-ray fields using independently measured source and geometry details *Med. Phys.* **36** 5622–32 %@ 0094-2405
- Schneider U, Agosteo S and Pedroni E 2002 Secondary neutron dose during proton therapy using spot scanning *Int. J. Radiat. Oncol. Biol. Phys.* **53** 244–51
- Schuemann J, Dowdell S, Grassberger C, Min C H and Paganetti H 2014 Site-specific range uncertainties caused by dose calculation algorithms for proton therapy *Phys. Med. Biol.* **59** 4007–31
- Seco J, Adams E, Bidmead M, Partridge M and Verhaegen F 2005 Head-and-neck IMRT treatments assessed with a Monte Carlo dose calculation engine *Phys. Med. Biol.* **50** 817
- Stovall M, Blackwell C R, Cundiff J and Novack D H 1995 Fetal dose from radiotherapy with photon beams: report of AAPM radiation therapy committee task group no. 36 *Med. Phys.* **22** 63–82
- Testa M, Schümann J, Lu H M, Shin J, Faddegon B, Perl J and Paganetti H 2013 Experimental validation of the TOPAS Monte Carlo system for passive scattering proton therapy *Med. Phys.* **40** 121719
- Wakeford R and Little M P 2003 Risk coefficients for childhood cancer after intrauterine irradiation: a review *Int. J. Radiat. Biol.* **79** 293–309
- Weisz B, Meirou D, Schiff E and Lishner M 2004 Impact and treatment of cancer during pregnancy *Expert Rev. Anticancer Ther.* **4** 889–902
- Willemse P, Van der Sijde R and Sleijfer D T 1990 Combination chemotherapy and radiation for stage IV breast cancer during pregnancy *Gynecol. Oncol.* **36** 281–4
- Wo J Y and Viswanathan A N 2009 Impact of radiotherapy on fertility, pregnancy, and neonatal outcomes in female cancer patients *Int. J. Radiat. Oncol. Biol. Phys.* **73** 1304–12
- Xu X G and Paganetti H 2010 Better radiation weighting factors for neutrons generated from proton treatment are needed *Radiat. Prot. Dosim.* **138** 291–4
- Xu X G, Taranenko V, Zhang J and Shi C 2007 A boundary-representation method for designing whole-body radiation dosimetry models: pregnant females at the ends of three gestational periods—RPI-P3, -P6 and -P9 *Phys. Med. Biol.* **52** 7023–44
- Zacharatou Jarlskog C, Lee C, Bolch W E, Xu X G and Paganetti H 2008 Assessment of organ-specific neutron equivalent doses in proton therapy using computational whole-body age-dependent voxel phantoms *Phys. Med. Biol.* **53** 693–717